THE JOURNAL OF BIOLOGICAL CHEMISTRY VOL. 287, NO. 34, pp. 28586–28597, August 17, 2012

α1- and α5-containing Laminins Regulate the Development of Bile Ducts via β1 Integrin Signals*[S]

Received for publication, February 6, 2012, and in revised form, June 24, 2012 Published, JBC Papers in Press, July 3, 2012, DOI 10.1074/jbc.M112.350488

Naoki Tanimizu[‡§1], **Yamato Kikkawa**[¶], **Toshihiro Mitaka**[‡], **and Atsushi Miyajima**[§]

From the [‡]*Department of Tissue Development and Regeneration, Research Institute for Frontier Medicine, Sapporo Medical University School of Medicine, S-1, W-17, Chuo-ku, Sapporo, 060-8556, Japan,* [¶]*Laboratory of Clinical Biochemistry, Tokyo University of Pharmacy and Life Sciences, Hachioji 192-0392, Japan, and* [§]*Institute of Molecular and Cellular Biosciences, The University of Tokyo, 1-1-1 Yayoi, Bunkyo-ku, Tokyo, 113-0032, Japan*

Background: Laminin isoforms are suggested to differentially regulate epithelial morphogenesis.
Results: Liver epithelial cells could not establish apicobasal polarity without laminin α1 or β1 integrin signal, whereas they formed immature lumen structures without laminin α5.
Conclusion: Laminins α1 and α5 are necessary to start and complete epithelial morphogenesis, respectively, during bile duct development.
Significance: Laminins α1 and α5 sequentially regulate different developmental processes to form epithelial tissues.

Signals derived from basal lamina components are important for developing three-dimensional architecture of epithelial tissues. Laminins consisting of α, β, and γ subunits in basal lamina play pivotal roles in the formation and maintenance of epithelial tissue structures. However, it remains unclear which laminin isoforms transmit signals and how epithelial cells receive them to regulate multiple developmental processes. In three-dimensional culture of a liver progenitor cell line, Hepatic Progenitor Cells Proliferating on Laminin (HPPL), the cells establish apicobasal polarity and form cysts with a central lumen. Neutralizing antibody against β1 integrin blocked the formation and maintenance of the cyst structure, indicating that β1 integrin signaling was necessary throughout the morphogenesis. Although the addition of α1-containing laminin, a ligand of β1 integrin, induced cyst formation, it was dispensable for the maintenance of the cyst, suggesting that HPPL produces another ligand for β1 integrin to maintain the structure. Indeed, we found that HPPL produced α5-containing laminin, and siRNA against laminin α5 partially inhibited the lumen formation. In fetal liver, p75NTR$^+$ periportal fibroblasts and bile duct epithelial cells, known as cholangiocytes, expressed α1- and α5-containing laminins, respectively. In laminin α5 KO liver, cholangiocytes normally emerged, but the number of bile ducts was decreased. These results suggest that α1-containing laminin is sufficient as a component of the basal lamina for the commitment of bipotential liver progenitors to cholangiocytes and the apicobasal polarization, whereas α5-containing laminin is necessary for the formation of mature duct structures. Thus, α1- and α5-containing laminins differentially regulate the sequential events to form epithelial tissues via β1 integrin signals.

Epithelial organs such as the lung, pancreas, kidney, and liver contain tissue structures such as acini, glands, and tubules to perform the functions of each organ. Epithelial apicobasal polarity in these tissue structures is essential for the directional transport of nutritional and metabolic substances in the liver, absorption of water and ions in the kidney, and gas exchange in the lung. The liver has two epithelial tissue structures, hepatic cords and bile ducts. Cholangiocytes, the epithelial cellular components of bile ducts, differentiate from hepatoblasts, bipotential liver progenitor cells, in midgestation and form tubular structures in the perinatal period (1, 2). Cholangiocytes first form ductal plates, epithelial cell layers around the portal vein, that are then reorganized into bile duct tubules. Recent studies revealed that the apical membrane is established at the early stage of bile duct morphogenesis (3, 4). Because abnormal development or degeneration of the apical lumina of bile ducts results in cholestasis that leads to liver failure (5), the formation and maintenance of the luminal space are crucial for performing the physiological roles of bile ducts.

Intracellular signals from either the apical or basal side of epithelial cells affect the formation and/or maintenance of the luminal structure of epithelial tissues. Cdc42 and phosphatase and tensin homolog on chromosome 10 (PTEN) are localized at the apical domain and segregate the apical domain in the plasma membrane to generate the apical lumen (6, 7). On the other hand, epithelial cells receive signals from extracellular matrix (ECM)[2] proteins on the basal side.

A major functional component in basal lamina is a laminin heterotrimer consisting of α, β, and γ chains (8, 9). Until now, five α, four β, and three γ chains, which are assembled into 18 different laminin isoforms, have been identified in mammals (10). Laminin isoforms are expressed differentially in a spatiotemporal manner and play substantial roles in the development of epithelial structures and functions (9). The expression of laminin isoforms in the normal and regenerating liver has been extensively studied (11, 12). In normal mouse and human adult

* This work was supported by a research grant from the Ministry of Education, Culture, Sports, Science, and Technology, Japan (to N. T., A. M., and T. M.).
[S] This article contains supplemental Figs. 1–7 and Movies 1 and 2.
[1] To whom correspondence should be addressed. Tel.: 81-11-611-2111 (ext. 2391); Fax: 81-11-615-3099; E-mail: tanimizu@sapmed.ac.jp.

[2] The abbreviations used are: ECM, extracellular matrix; CK, cytokeratin; EpCAM, epithelial cell adhesion molecule; HPPL, Hepatic Progenitor Cells Proliferating on Laminin; PECAM, platelet endothelial cell adhesion molecule; E, embryonic day; P, postnatal day; aPKC, atypical protein kinase C.

livers, α5-containing laminins, which are laminins 511 (α5β1γ1) and 521 (α5β2γ1), were strongly expressed in basal lamina underlying portal and central veins, hepatic arteries, and bile ducts, whereas in regenerating mouse liver after two-thirds partial hepatectomy, α1-containing laminin, which is laminin 111 (α1β1γ1), was transiently expressed in liver lobules. Furthermore, in the developing liver, the basal lamina including laminin was detected around the liver bud and also around bile ducts at a later stage in development (13). However, it has not been determined which laminin isoforms are expressed at different stages of liver organogenesis. We have reported previously that α1-containing laminin (laminin 111) is essential for the bipotential liver progenitor cell line HPPL to develop apicobasal polarity and cholangiocyte characteristics in three-dimensional culture (14). Although our results indicated that laminin was essential for liver epithelial cells to establish the polarity and lumen as cholangiocytes, it has remained unknown how HPPL receives signals from α1-containing laminin and which cells provide laminin *in vivo* during bile duct development.

Integrin, a heterodimer consisting of α and β chains, is a major receptor for ECM proteins including laminins. Among the subunits, β1 chain has been shown to be required for developing appropriate tissue structures both *in vivo* and *in vitro* (15–18). A recent study showed that β1 integrin could mediate distinct signals by associating with different α subunits during epithelial morphogenesis (19). However, it remains unknown which type of laminin isoform is important as a ligand for β1 integrin to regulate a specific step of epithelial tissue morphogenesis. Furthermore, the roles of β1 integrin in the formation of liver tissue architecture have not been studied yet.

In this study, we investigated the expression and function of laminin isoforms containing α1 and α5 chains in bile duct development. By using neutralizing antibody against β1 integrin and siRNA against laminin α5, we addressed the roles of these laminin isoforms in cyst morphogenesis in three-dimensional culture. We also addressed the roles of α1- and α5-containig laminins *in vivo* by demonstrating the normal emergence of cholangiocytes and the abnormal morphogenesis of bile ducts in laminin α5 knock-out mice. Our results indicate that liver epithelial cells sequentially utilize α1- and α5-containing laminins as ligands for β1 integrin in distinct processes of bile duct morphogenesis, revealing the functional significance of the transition from α1- to α5-containing laminin, which occurs widely in the basal lamina of developing epithelial tissues.

EXPERIMENTAL PROCEDURES

ECM Proteins and Growth Factors—Type I collagen was purchased from Koken Co., Ltd. (Tokyo, Japan). Growth factor-reduced Matrigel and purified laminin 111 were from BD Biosciences. Recombinant laminin 511 was produced in HEK293 cells triply transfected with mouse laminin α5, β1, and γ1 chains and purified as described previously (20). Epidermal growth factor (EGF) and hepatocyte growth factor were from Invitrogen and R&D Systems (Minneapolis, MN), respectively.

Culture of HPPL in Two- and Three-dimensional Conditions—HPPL was kept in DMEM/F-12 (Sigma) containing 10% FBS (Invitrogen), 1× insulin/transferrin/selenium (Invitrogen), 10 mM nicotinamide (Wako, Osaka, Japan), 0.1 μM dexamethasone (Sigma), 5 mM L-glutamine, and 5 ng/ml hepatocyte growth factor and EGF. To induce the formation of cyst structures, we modified the method reported previously (14). The bottom layer of culture was prepared in each well of 8-well coverglass chambers (Nunc, Roskilde, Denmark) by adding 50 μl of a 1:1 mixture of Matrigel and type I collagen solution. HPPL (3×10^3 cells in 150 μl of medium) was plated on the bottom layer. After 10 min of incubation, the cells were covered with 10% Matrigel in DMEM/F-12 containing growth factors. At day 4 of the culture, the upper layer of Matrigel was replaced with fresh DMEM/F-12 containing 5% Matrigel and growth factors.

Transfer of Cysts from Matrigel to Type I Collagen Gel—HPPL was kept in 5% Matrigel for 4 days in a well of a coverglass chamber to allow the cells to generate cyst structures. After washing with PBS, ice-cold Cell Recovery Solution (BD Biosciences) was added to the well. The chamber was put on ice for 1 h. The whole solution was transferred to a 15-ml tube and then centrifuged at 1,200 rpm for 4 min. The pellet containing cysts was resuspended in type I collagen solution and poured into a 1-cm-diameter tissue culture insert (0.02-μm Anopore membrane, Nunc). HPPL cysts were kept in type I collagen gel for 3 additional days before immunocytochemical analysis.

Blocking Interactions between HPPL and Laminins in Three-dimensional Culture—Neutralizing antibodies against β1 integrin (clone Ha2/5, BD Biosciences), α6 integrin (clone GoH3, Biolegend, San Diego, CA), and αV integrin (clone RMV-7, Biolegend) were used at a final concentration of 50 μg/ml to block the interaction between HPPL and ECM components. Hamster IgM (BD Biosciences) and rat IgG (Biolegend) were used as controls. Antibodies were added from the beginning or at day 4 of three-dimensional culture. Three thousand cells suspended in 150 μl of DMEM/F-12 containing growth factors were plated into each well of an 8-well coverglass chamber (Nunc) coated with a mixture of type I collagen and Matrigel. Ten minutes after plating, 150 μl of 10% Matrigel containing control IgM, control IgG, or neutralizing antibody was added and mixed by gently tapping. When antibody was added at day 4 of the culture, wells were added with 400 μl of ice-cold Cell Recovery Solution (BD Biosciences) and incubated on ice for 30 min. After washing with medium, 200 μl of fresh medium containing 5% Matrigel, growth factors, and IgM, IgG, or neutralizing antibody was added to each well.

Knockdown of Laminin α5—piLenti plasmids containing target sequences were purchased from Applied Biological Materials Inc. (Richmond, British Columbia, Canada). piLenti, pRev, and pGag plasmids were co-transfected into 293T cells. Culture medium containing lentivirus particles was diluted with fresh medium containing growth factors and added to HPPL. After 3 days, the medium was replaced with fresh medium containing 1 μg/ml puromycin. After selecting puromycin-resistant cells, the expression of laminin α5 was examined by quantitative PCR.

Culture of Hepatoblasts—Hepatoblasts were isolated from E14.5 liver based on expression of Dlk1 as reported previously (21). Cells were plated on dishes coated with either laminin 111 or recombinant laminin 511 and kept in the same medium used

TABLE 1
Primary antibodies used for immunostaining

Antigen	Company or source	Host	Dilution
E-cadherin	BD Transduction Laboratories	Mouse	1:1,500
β-Catenin	BD Transduction Laboratories	Mouse	1:1,500
Cytokeratin 19	Tanimizu *et al.* (21)	Rabbit	1:2,000
EpCAM	BD Pharmingen	Rabbit	1:500
α6 integrin	Biolegend	Rat	1:500
β1 integrin	Chemicon	Rat	1:500
β4 integrin	BD Pharmingen	Rat	1:500
HNF4α	Santa Cruz Biotechnology	Goat	1:200
Laminin α1	A gift from Dr. Takako Sasaki (Oregon Health and Science University)	Rabbit	1:2,000
Laminin α5	A gift from Dr. Takako Sasaki (Oregon Health and Science University)	Rabbit	1:2,000
Protein kinase ζ	Santa Cruz Biotechnology	Rabbit	1:100
Sox9	Millipore	Rabbit	1:500
ZO1	Zymed Laboratories Inc.	Rabbit	1:200
ZO1	A gift from Dr. Bruce Stevenson (University of Alberta)	Rat	1:2,000

for HPPL. After 3 days, the culture medium was replaced with serum-free DMEM/F-12 containing 500 pg/ml TGFβ. After 24 h of stimulation, cells were dissolved in a lysis buffer and used for RNA preparation.

Immunofluorescence Microscopy—Mouse embryonic and neonatal livers were fixed in PBS containing 4% paraformaldehyde at 4 °C, embedded in optical cutting temperature compound (OCT) compound, and frozen. Laminin α5 KO livers were kindly provided by Dr. Jeff H. Miner (Washington University, St. Louis, MO). They were used for preparation of thin sections using a cryostat (Leica, St. Gallen, Switzerland). Serial sections along the cranial tail axis were prepared from three homozygous mutant and two heterozygous livers. To count the number of duct structures and measure the lumen size, $CK19^+$ structures around the portal veins were examined in more than 10 sections at different locations along the axis from the liver hilum to the periphery. Samples of the culture were gently washed with PBS and then fixed in paraformaldehyde solution. After incubation in PFS (PBS containing 7% cold water fish gelatin (Sigma) and 0.1% saponin (Sigma)) at 4 °C for 30 min, primary antibodies diluted in PFS were added to each well. To remove excess antibodies, samples were gently washed with PBS. Primary antibodies used in this study are listed in Table 1. Signals were visualized with Alexa Fluor-conjugated secondary antibodies (Molecular Probes, Eugene, OR) used at a dilution of 1:500. F-actin bundles were detected with Alexa Fluor 488-, 555-, or 633-conjugated phalloidin (Molecular Probes) at a dilution of 1:250. Nuclei were counterstained with Hoechst 34580. Samples were examined using Zeiss LSM 510 and Olympus FV1000D IX81 confocal laser-scanning fluorescence microscopes.

Live Cell Imaging—HPPL expressing YFP-actin was kept in 5% Matrigel for 4 days in a 2-well coverglass chamber (Nunc). After exchanging the upper layer with fresh medium containing 5% Matrigel and either hamster IgM or anti-β1 integrin antibody (Ha2/5), the coverglass chamber was set on the stage of an Olympus FV1000 IX81 microscope. The temperature and CO_2 concentration were kept at 37 °C and 5%, respectively. Fifteen points were selected and followed for 24 h. Every 40 min, an X-Y image was captured at each point.

Cell Isolation and Quantitative PCR—E14.5 liver cells were labeled with FITC-conjugated rat monoclonal anti-Dlk1 (22), phycoerythrin-conjugated rat monoclonal anti-PECAM (Biolegend), allophycocyanin-conjugated rat monoclonal anti-p75NTR (23), allophycocyanin/Cy7-conjugated rat monoclonal anti-CD45 (Biolegend), and allophycocyanin/Cy7-conjugated rat monoclonal anti-TER119 (Biolegend) antibodies. E17.5 liver cells were labeled with FITC-conjugated rat monoclonal anti-EpCAM (24) and phycoerythrin-conjugated rat monoclonal anti-ICAM1 (BD Biosciences) antibodies. Postnatal day 0 (P0) liver cells and adult liver nonparenchymal cells were labeled with the FITC-conjugated anti-EpCAM antibody. Cells were fractionated on a FACSvantage SE or FACSAria (BD Biosciences). Isolated cells were used for RNA isolation followed by cDNA synthesis using Omniscript reverse transcriptase (Qiagen, Dusseldorf, Germany). PCR was performed on an ABI Prism 7500 (Applied Biosystems Inc., Foster City, CA) with TaqMan gene expression assays for mouse laminins α1 and α5 and hypoxanthine phosphoribosyltransferase. The threshold cycle (Ct) for each sample was determined on the ABI Prism software. We used the comparative Ct method to compare expression levels of laminin α chains among liver cell fractions using hypoxanthine phosphoribosyltransferase as an internal control and P0 kidney as a calibrator sample. The relative expression level was determined as the value of $2^{-\Delta\Delta Ct}$. ΔCt and ΔΔCt were determined by using the following formulas: ΔCt (a liver cell fraction) = Ct (laminin α1 or α5) − Ct (hypoxanthine phosphoribosyltransferase) and ΔΔCt = ΔCt (a liver cell fraction) − ΔCt (P0 kidney).

RESULTS

β1 Integrin Signal Is Necessary for Liver Progenitor Cells to Develop and Maintain the Cyst Structure—HPPL forms cysts with a central lumen in three-dimensional culture (14). Because β1 integrin was expressed at the basal domain of HPPL throughout cyst morphogenesis in culture (Fig. 1*A*), we considered the possibility that β1 integrin transmits signals from the ECM for liver progenitor cells to develop apicobasal polarity and lumen. To test whether the interaction between ECM and β1 integrin is required for the development of cyst structures, we used a neutralizing anti-β1 integrin monoclonal antibody (clone Ha2/5). The addition of the anti-β1 antibody from the beginning of three-dimensional culture (Fig. 1*B*) remarkably inhibited the lumen formation (Fig. 1*C*). In the control culture, HPPL formed cysts with polarity markers at their proper locations (Fig. 1*D*, *upper panels*); apical markers atypical protein kinase C (aPKC) (Fig. 1*D*, *panel 2*) and F-actin (Fig. 1*D*, *panel 3*) were localized at the apical membrane, whereas α6 integrin was

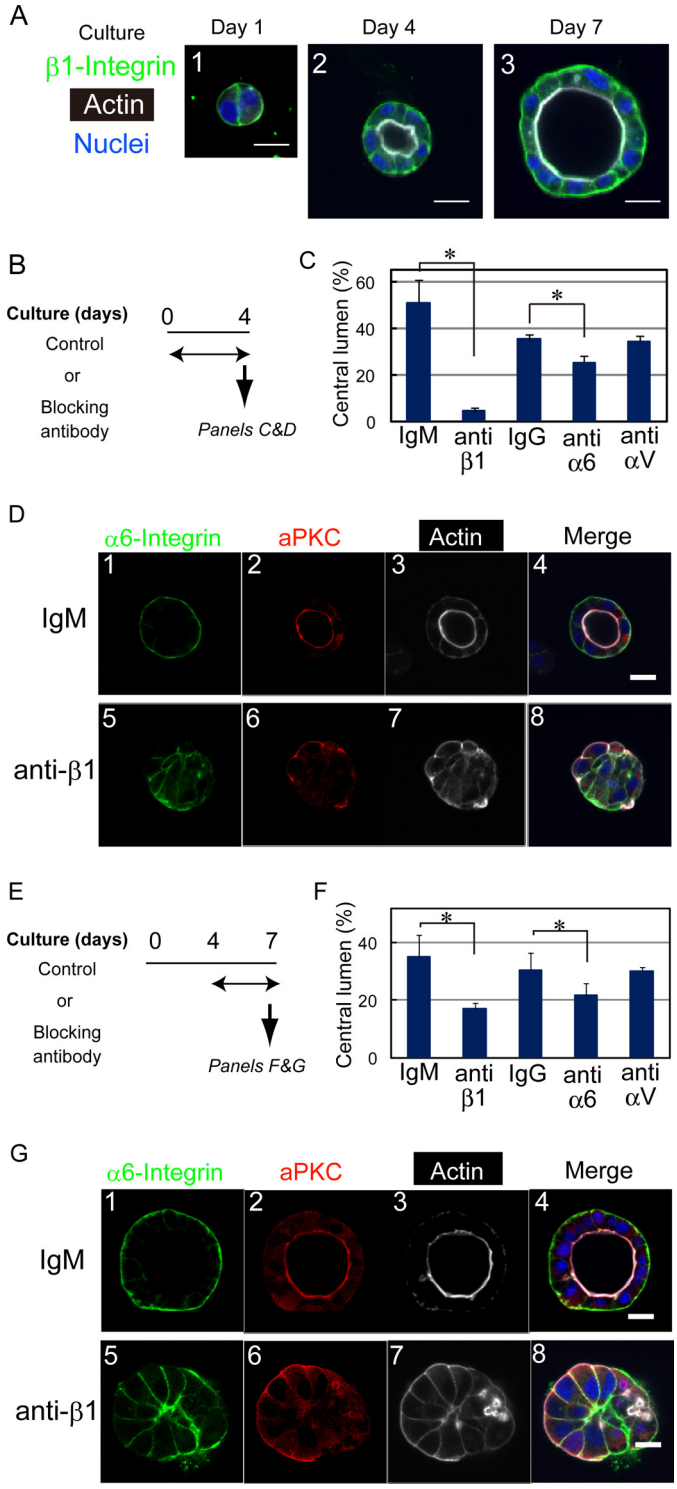

FIGURE 1. **β1 integrin is necessary for HPPL to develop and maintain the cyst structure.** *A*, expression of β1 integrins during three-dimensional culture. β1 integrin is clearly localized at the basolateral domain throughout the culture. Cysts were stained with anti-β1 integrin antibody, which was visualized with Alexa Fluor 488-conjugated anti-rat IgG and Alexa Fluor 633-conjugated phalloidin. The *bar* represents 20 μm. *B*, timetable for the addition of the anti-β1 integrin (clone Ha2/5), anti-α6 integrin (clone GoH3), or anti-αV integrin (clone RMV7) antibody to three-dimensional culture to examine roles of laminin-integrin interactions in the development of the cyst structure. One of those blocking antibodies was added to three-dimensional culture from the beginning, the lumen formation was examined as shown in *C*, and immunofluorescence analysis was performed at day 4 as shown in *D*. *C*, anti-β1 and -α6 antibodies decrease the number of cysts with a central lumen. The number of cellular structures with or without lumen was counted under a microscope. Cultures were repeated three times independently. More than 200 cellular structures in each well were examined. A *t* test was performed by Microsoft Excel software. *, $p < 0.05$. *D*, HPPL forms cell aggregates in the presence of the anti-β1 integrin antibody. In the control culture, aPKC (*D*, *panel 2*) and F-actin (*D*, *panel 3*) are localized at the apical domain, and α6 integrin (*D*, *panel 1*) is at the basolateral domains. In the presence of the anti-β1 antibody, aPKC (*D*, *panel 6*) and F-actin (*D*, *panel 7*) are localized at the boundary between cells and the ECM gel, whereas α6 integrin (*D*, *panel 5*) remains at the lateral domain but is excluded from the basal domain. *E*, timetable for the addition of the anti-β1, -α6, or -αV integrin monoclonal antibody to three-dimensional culture to examine the roles of the interaction in the maintenance of the cyst structure. One of the antibodies was added to three-dimensional culture at day 4, and the culture was terminated at day 7 for counting the number of cysts (*F*) and for immunofluorescence analysis (*G*). *F*, the number of cysts with a central lumen is decreased in the presence of anti-β1 or anti-α6 antibody. The number of cellular structures with or without lumen was counted at day 7 under a microscope. Cultures were repeated three times independently. More than 200 cellular structures in each well were examined. A *t* test was performed by Microsoft Excel software. *, $p < 0.05$. *G*, the cyst structure of HPPL is disrupted by the addition of the anti-β1 integrin antibody. aPKC (*G*, *panel 2*) and F-actin (*G*, *panel 3*) are localized at the apical domain, whereas α6 integrin (*G*, *panel 1*) is found at the basolateral domain in the control. By the addition of the anti-β1 antibody, the localization of aPKC (*G*, *panel 6*) and F-actin (*G*, *panel 7*) changes from the apical domain to near the ECM, whereas α6 integrin remains at the lateral domain but is excluded from the basal domain (*G*, *panel 5*). *Error bars* in *panels C* and *F* represent standard deviation. *Bars* represent 20 μm.

localized at the basal domain (Fig. 1*D*, *panel 1*). In contrast, in the presence of the anti-β1 antibody, HPPL formed cell aggregates without lumen (Fig. 1*D*, *lower panels*). In those cell aggregates, aPKC (Fig. 1*D*, *panel 6*) and F-actin (Fig. 1*D*, *panel 7*) were localized at the boundary between the cells and ECM. α6 integrin was localized at the cell-cell boundary but was absent at the boundary between cells and ECM (Fig. 1*D*, *panel 5*). We also added anti-α6 or anti-αV antibody to three-dimensional culture and found that anti-α6 antibody significantly inhibited the formation of cysts (Fig. 1*C*).

Next, to examine whether the β1 integrin signal is also important for maintaining the cyst structure, we added anti-β1 integrin antibody to the culture from day 4 of the culture and incubated it for an additional 3 days (Fig. 1*E*). Anti-β1 antibody reduced the number of cysts with a central lumen (Fig. 1*F*). Immunocytochemical analysis showed the altered localization of polarity markers in the presence of anti-β1 antibody; aPKC (Fig. 1*G*, *panel 6*) and F-actin bundles (Fig. 1*G*, *panel 7*) were localized at the boundary between the cells and ECM gel, whereas α6 integrin was excluded from the boundary (Fig. 1*G*, *panel 5*). We also added anti-α6 or anti-αV antibody to the culture from day 4 and found that anti-α6 antibody reduced the number of cysts (Fig. 1*F*).

β4 integrin, which is another β subunit expressed in HPPL, was detected at the basal surface of HPPL after the establishment of the apicobasal polarity (supplemental Fig. 1A). During the bile duct development, β4 integrin expression was observed from a later stage as compared with β1 integrin (supplemental Fig. 2). Based on these data, we considered the possibility that β4 integrin is involved in the maintenance of the cyst structure. We added a neutralizing antibody against β4 integrin from day 4 of the culture. The number of cysts was only slightly decreased in the presence of anti-β4 antibody (supplemental Fig. 1C), suggesting that it is not a major receptor mediating signals to HPPL for the maintenance of the cyst structure. These data indicated that the β1 integrin signal is required for

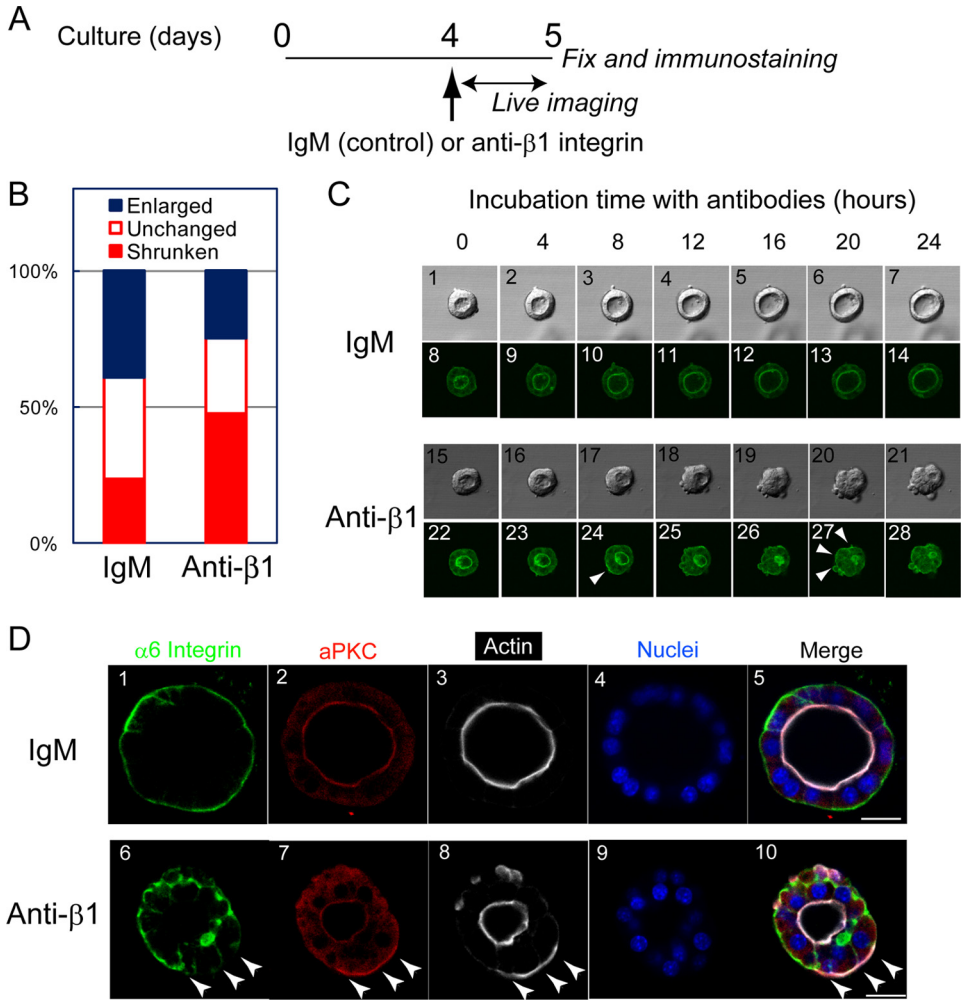

FIGURE 2. **Live cell imaging shows the processes of loss of normal polarity and collapse of the central lumen in the presence of anti-β1 integrin antibody.** *A*, timetable for live cell imaging and immunofluorescence. HPPL expressing YFP-actin was cultured in Matrigel for 4 days. After changing the upper layer to 5% Matrigel containing an anti-β1 integrin antibody, the plate was placed on a microscope, and images were acquired every 40 min in the following 24 h. *B*, the apical lumens of the cysts were categorized into three groups: enlarged, unchanged, and shrunken. The ratio of "shrunken" lumen was significantly increased in the presence of the anti-β1 integrin antibody as compared with the control. *C*, images taken every 4 h during live imaging are shown. Typically, HPPL exhibited a slightly expanded central lumen in the presence of control IgM (*panels 1–14*), whereas they lost apical localization of YFP-actin and the central lumen in the presence of the anti-β1 integrin antibody (*panels 15–28*). *D*, localization of apical and basal markers was examined at 24 h after the addition of the antibodies. When the central lumen still remained, apical markers such as aPKC and F-actin were evident at the basal domain (*D*, *panels 7* and *8*, *arrowheads*). In contrast, α6 integrin was excluded from the basal domain of the cells showing basal aPKC and F-actin (*D*, *panel 6*). *Scale bars* represent 20 μm.

both development and maintenance of the cyst structure and that α6 integrin is a crucial partner of β1 integrin.

Live Cell Imaging Shows a Link between Dissolution of Polarity and Collapse of the Central Lumen—The results using the anti-β1 integrin antibody showed that the interaction between β1 integrin and laminin is important for the maintenance of the cyst structure (Fig. 1*E*-G). However, immunofluorescence images at specific time points of three-dimensional culture did not reveal the entire picture of how blocking the laminin-integrin interaction disrupted the cyst structure. To visualize changes of the cyst structure by blocking the interaction between β1 integrin and laminin, a confocal microscope was used to monitor the cyst structure in three-dimensional culture for 24 h after the addition of the anti-β1 integrin antibody (Fig. 2*A*). Because F-actin bundles are an excellent indicator of polarity and lumen, we established HPPL cells expressing YFP-actin to visualize F-actin localization in live cells. We confirmed that YFP-actin was localized at the apical regions of cysts (Fig. 2*C*, *panels 8* and *22*). We monitored the size of the central lumen during incubation and classified the lumens into three types: enlarged, unchanged, and shrunken (or collapsed in some cases). Enlarged and shrunken cysts were observed most frequently in the absence and presence of the anti-β1 integrin antibody, respectively (Fig. 2*B*). Fig. 2*C*, *panels 1–14* (supplemental Movie 1) and *15–28* (supplemental Movie 2) show representative morphologies of enlarged and shrunken cysts in the presence and absence of anti-β1 integrin antibody, respectively. At 8 h after the addition of the antibody, YFP-actin appeared near the ECM (Fig. 2*C*, *panel 24*, *arrowhead*). At this time, the central lumen with an intense YFP-actin signal was still observed, although it had started to shrink. Beyond that time, basal actin became gradually evident (Fig. 2*C*, *panel 27*, *arrowheads*), and the lumen shrunk further and eventually collapsed. We then characterized cysts in culture by immunofluorescence staining at 24 h after the addition of the anti-β1 integrin antibody. At this time point, some cysts were still losing their polar-

ity and lumen. Even when the central lumen remained, aPKC and F-actin were localized near the ECM in some cells, whereas α6 integrin was excluded from the basal domain (Fig. 2*D*, *panels 6*, *7*, and *8*, *arrowheads*). These results suggested that the central lumen collapsed sequentially; at first, the interaction between laminin and β1 integrin was lost followed by dissolution of the apical proteins, and finally the central lumen collapsed.

Exogenous α1-containing Laminin Is Dispensable for Maintenance of the Cyst Structure—Because exogenous α1-containing laminin is needed for HPPL to form cysts (14), it was likely to be a major ligand for β1 integrin during the formation of cysts (Fig. 3*A*). However, it remained unknown whether exogenous α1-containing laminin is required after the formation of cysts. To address this question, we isolated cysts from Matrigel, the source of the α1-containing laminin, at day 4 and embedded them in type I collagen gel (Fig. 3*B*). Unexpectedly, even though α1-containing laminin was removed from the cysts (Fig. 3*C*, *panel 1*), the apicobasal polarity and the central lumen were maintained in the collagen gel (Fig. 3*C*, *panel 2*). This result indicated that exogenous α1-containing laminin was no longer required for the maintenance of the cyst structure, whereas β1 integrin signaling was required for the maintenance, suggesting that HPPL might produce laminins during cyst formation.

α5-containing Laminin Is Produced from HPPL and Integrated into an ECM Layer during Cyst Formation and Contributes to Expand the Lumen—To address the possibility that HPPL produces laminins, we examined the expression of laminin α chains in HPPL both in two-dimensional and three-dimensional culture conditions and found that HPPL expressed laminin α5 mRNA in both culture conditions (Fig. 3*D*). HPPL also expressed laminin β2 and γ1 chain mRNAs, indicating that the α5-containing laminin produced by HPPL was laminin 521. By immunostaining, we also examined whether HPPL expressed laminin α5 protein during cyst formation (Fig. 3*E*). At day 2 when the lumen was being developed, laminin α5 was detected at the boundary between the basal domain of cells and surrounding gel (Fig. 3*E*, *panels 1–4*). At day 4 when F-actin bundles lined the central lumen, laminin α5 was localized at the basal domain (Fig. 3*E*, *panels 5–8*). Basal laminin α5 was also observed at day 7 of culture (Fig. 3*E*, *panels 9–12*). These results suggested that α5-containing laminin was produced by HPPL and integrated into the ECM layer around cysts, contributing to the maintenance of the cyst structure.

To address the roles of α5-containing laminin in epithelial morphogenesis, we introduced siRNA against laminin α5 to HPPL and generated HPPL with reduced expression of laminin α5 (HPPL-siLamα5; supplemental Fig. 3). In three-dimensional culture, HPPL-siLamα5 formed cysts with a lumen, although the central lumen looked smaller than that of the control (Fig. 3*F*). We further measured the lumen diameter of cysts derived from HPPL-siLamα5 as well as those from the control. The result indicated that cysts derived from HPPL-siLamα5 had a significantly smaller lumen than those from the control at day 4 (Fig. 3*G*). Less extension of the apical membrane in HPPL-siLamα5 might be a reason for the formation of a smaller lumen (supplemental Fig. 4). These results suggested that endogenous α5-containing laminin is dispensable for establishing apico-

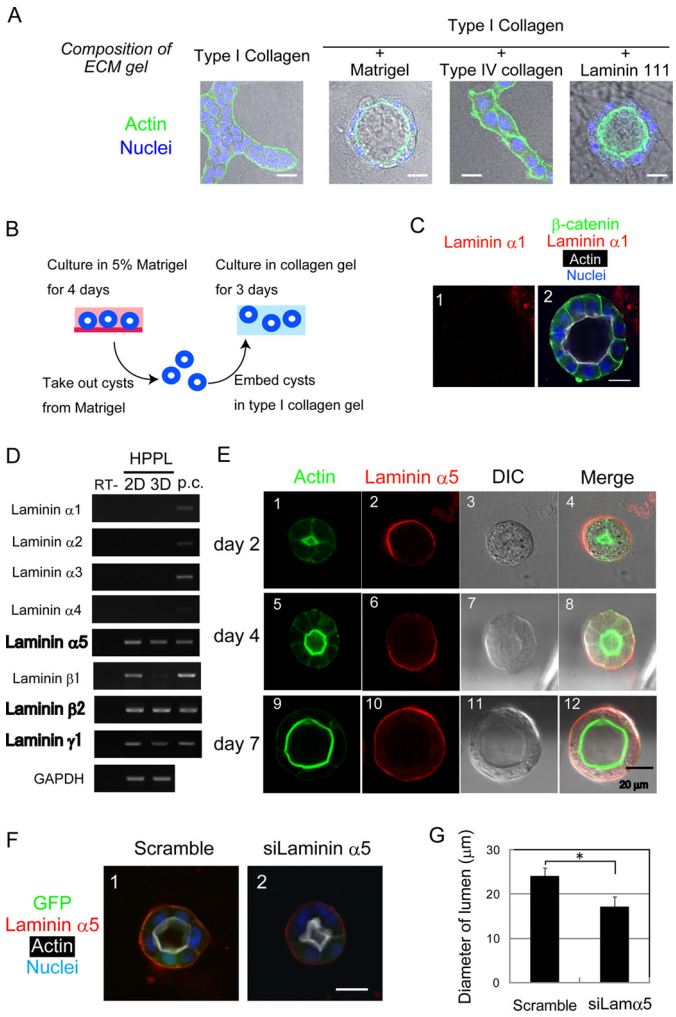

FIGURE 3. **HPPL produces α5-containing laminin.** *A*, HPPL forms cysts depending on laminin 111 (α1-containing laminin). HPPL was cultured in type I collagen gel or type I collagen gel containing 40% Matrigel, 40% type IV collagen, or 40% laminin 111. HPPL formed cysts in the presence of Matrigel or laminin 111. Cells were stained with Alexa Fluor 488-conjugated phalloidin and Hoechst 34580. *B*, a schematic view of the experiment to examine whether α1-containing laminin is crucial for HPPL to maintain the apicobasal polarity and lumen. HPPL was cultured in the presence of Matrigel for 4 days to form cysts. HPPL cysts were isolated from Matrigel by incubation in Cell Recovery Solution on ice for 1 h and then embedded in type I collagen gel. After incubation for 3 days in collagen gel, localization of β-catenin, laminin α1, and F-actin was examined. *C*, the cyst structure is maintained without exogenous α1-containing laminin. β-Catenin (*green*) and F-actin (*white*) are localized at the basolateral and apical domains, respectively, and the central lumen is maintained in type I collagen gel. The *bar* represents 20 μm. *D*, HPPL expresses laminins α5, β2 and γ1 in two-dimensional and three-dimensional culture. Expression of all the α chain, β1 and β2, and γ1 mRNAs was examined by RT-PCR. The α5, β2, and γ1 chains are expressed both in two-dimensional and three-dimensional culture, whereas the β1 chain is expressed in two-dimensional but not in three-dimensional culture. First strand cDNA synthesized from P8 kidney lysate was used as the positive control (*p.c.*). *E*, laminin α5 protein produced by HPPL accumulates at the basal surface of cysts. At day 2, F-actin is accumulated at the apical membrane of the developing central lumen. Laminin α5 is detected at the boundary between cells and Matrigel (*panels 1–4*). At days 4 and 7, HPPL cells develop an apical lumen surrounded by thick F-actin bundles, indicating that they have established apicobasal polarity. At these time points, laminin α5 is detected clearly at the basal surfaces of cysts (*panels 5–12*). *F* and *G*, HPPL-siLamα5 (HPPL expressing siRNA against laminin α5) forms smaller cysts as compared with the control. The control and HPPL-siLamα5 were cultured for 4 days. HPPL-siLamα5 forms a cyst with the central lumen surrounded by F-actin bundles (*white*), but the lumen size is smaller than that of the control cyst (*F*). The lumen diameter of cysts derived from HPPL-siLamα5 is statistically significantly shorter than that derived from the control HPPL (*G*). *Error bars* represent standard deviation. *DIC*, differential interference contrast.

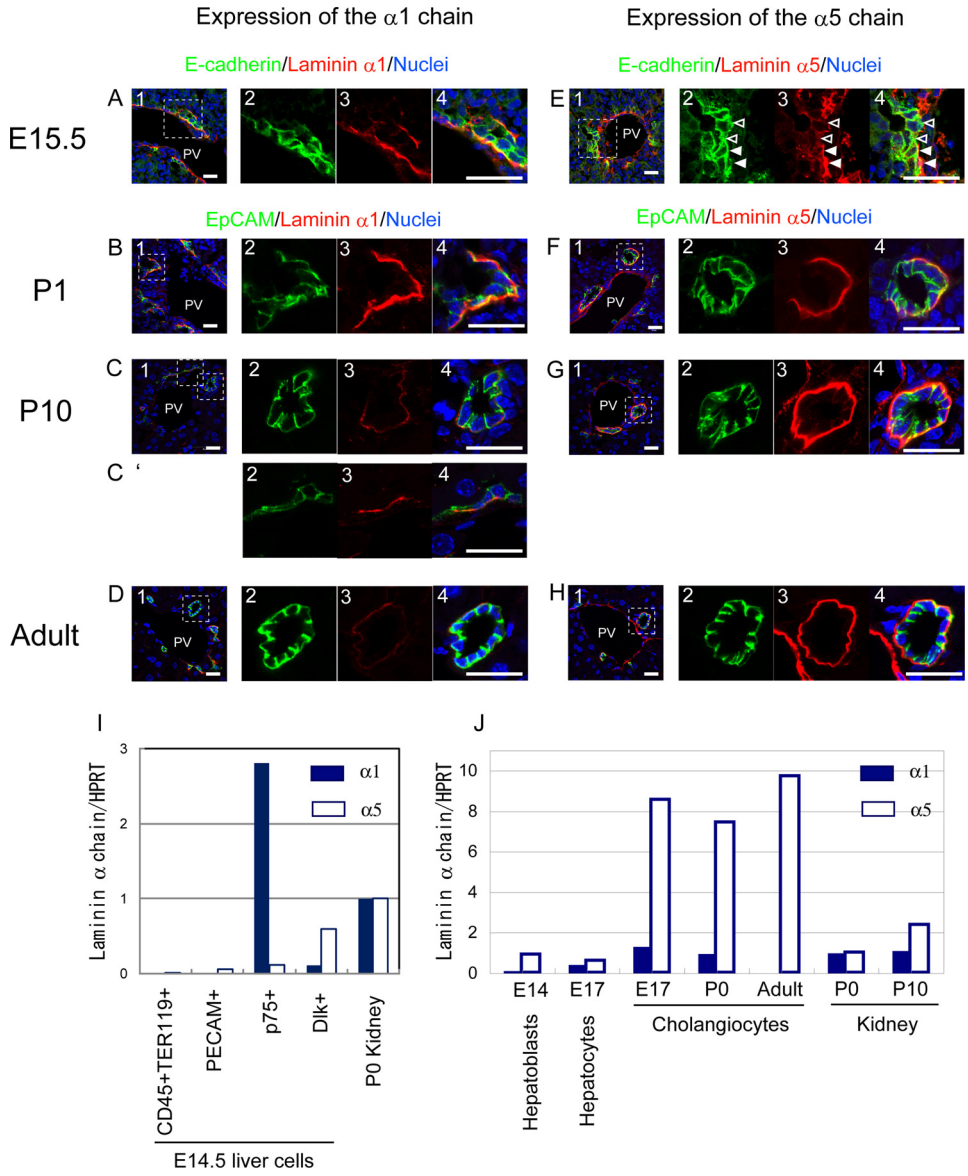

FIGURE 4. **Distribution of laminins α1 and α5 in developing liver.** *A–D*, laminin α1 is detected at the basal side of E-cadherin$^+$ cholangiocytes forming a ductal plate in E15.5 (*A*, *panels 1–4*) and EpCAM$^+$ cholangiocytes in the P1 liver (*B*, *panels 1–4*), whereas its expression is dramatically reduced in the P10 liver (*C*, *panels 1–4*) and then disappears from the basal side of cholangiocytes forming mature bile ducts in the adult liver (*D*, *panels 1–4*). In the P10 liver, α1 is still observed at the basal side of the remaining ductal plate (*C′*, *panels 2–4*). *Bars* represent 20 μm. *E–H*, laminin α5 is detected at the basal side of most of the E-cadherin$^+$ cholangiocytes in E15.5 (*E*, *panels 1–4*), although it is excluded from the basal side of some cholangiocytes (*open arrowheads*). In the P1 liver, laminin α5 is clearer at the basal side of cholangiocytes (*F*, *panels 1–4*). Later, laminin α5 is abundantly present at the basal side of cholangiocytes in P10 (*G*, *panels 1–4*) and adult liver (*H*, *panels 1–4*). *Bars* represent 20 μm. *I*, expression of laminins α1 and α5 by various types of cells at E14.5. Hematopoietic (CD45$^+$TER119$^+$) and endothelial (PECAM$^+$) cells, progenitors of stellate and periportal fibroblasts (p75NTR$^+$), and hepatoblasts (Dlk$^+$) were isolated from the E14.5 fetal liver when hepatoblasts near the portal vein were undergoing differentiation to cholangiocytes. p75NTR$^+$ cells express the α1 chain, whereas Dlk$^+$ cells weakly express the α5 chain. The levels of α1 and α5 chains are presented in this graph as the ratio against the expression level of each α chain in the P0 kidney. *J*, expression of laminins α1 and α5 during differentiation along the cholangiocyte lineage. Laminin α1 increased 5-fold in E17 cholangiocytes as compared with E14 hepatoblasts. However, the expression of laminin α1 mRNA was transient; it decreased in P1 cholangiocytes and then disappeared in adult cholangiocytes. On the other hand, laminin α5 increased 9-fold in E17 cholangiocytes as compared with E14 hepatoblasts, and the strong expression of laminin α5 was maintained in neonatal and adult cholangiocytes. The expression of α1 and α5 chains in Dlk$^+$ hepatoblasts, ICAM1$^+$ hepatocytes, and EpCAM$^+$ cholangiocytes isolated from the developing liver was examined by quantitative PCR. The levels of α1 and α5 chains are presented in the graph as the ratio against the expression level of each α chain in the P0 kidney. *HPRT*, hypoxanthine phosphoribosyltransferase; *PV*, portal vein.

basal polarity and lumen but does contribute to expand the apical lumen.

Expression of Laminins α1 and α5 in Vivo during Bile Duct Morphogenesis—It has been well established that cholangiocytes are associated with the laminin layer from the onset of their differentiation (13). However, it has remained unknown which laminin α chain is the major component at each specific developmental stage. We performed immunostaining of fetal, neonatal, and adult livers with antibodies against laminins α1 and α5 (Fig. 4). EpCAM staining clearly marks cholangiocytes beyond E17.5, and intensive E-cadherin staining at cell-cell contacts is a marker of newly differentiated cholangiocytes at E15.5 or E16.5 (3). At E15.5, laminin α1 was clearly detected at the basal side of E-cadherin$^+$ cholangiocytes in the ductal plate (Fig. 4*A*). Laminin α5 was also detected at the basal side of cholangiocytes (Fig. 4*E*, *closed arrowheads*). In contrast to

laminin α1, cholangiocytes without basal laminin α5 were also observed at E15.5 (Fig. 4*E*, *open arrowheads*). (About 25% of E-cadherin$^+$ cholangiocytes were not associated with laminin α5, whereas less than 10% of them were not associated with laminin α1.) Just after birth (P1), cholangiocytes were associated with both α1 and α5 chains (Fig. 4, *B* and *F*). At P10, cholangiocytes constituting bile duct tubules were associated only with the α5 chain (Fig. 4, *C* and *G*), whereas laminin α1 was still detected at the basal side of cholangiocytes in the remnants of ductal plates (Fig. 4*C′*). In the adult liver, cholangiocytes in bile ducts were associated only with the laminin α5 chain (Fig. 4, *D* and *H*) as observed at P10. Thus, both α1 and α5 chains were localized beneath cholangiocytes during tubular morphogenesis, whereas the α1 chain disappeared after the completion of tubular morphogenesis.

To confirm which types of cells produced α1 and α5 chains, we first isolated CD45$^+$TER119$^+$ hematopoietic cells, PECAM$^+$ endothelial cells, p75NTR$^+$ fibroblasts (23), and Dlk1$^+$ hepatoblasts (21) from E14.5 livers and examined the expression of laminins α1 and α5 by quantitative PCR (Fig. 4*I*; the purity of Dlk1$^+$ hepatoblasts and p75NTR$^+$ cells was confirmed by quantitative PCR as shown in supplemental Fig. 5). We also isolated Dlk1$^+$ hepatoblasts and EpCAM$^+$ cholangiocytes from developing and adult livers and examined the expression of laminins α1 and α5 by quantitative PCR (Fig. 4*J*). The data showed that p75NTR$^+$ cells including periportal fibroblasts expressed the laminin α1 chain, whereas EpCAM$^+$ cholangiocytes expressed the laminin α5 chain strongly but the α1 chain only weakly. Thus, α1-containing laminin was provided to liver epithelial cells mainly from adjacent cells in a juxtacrine fashion, whereas α5-containing laminin was produced by liver epithelial cells when they differentiated along the cholangiocyte lineage.

Loss of Laminin α5 Does Not Affect the Lineage Determination of Hepatoblasts—To determine whether α5-containing laminin had any specific function in the development of bile ducts *in vivo*, we compared E17.5 livers derived from laminin α5-null mice with those from heterozygous mice (Fig. 5). At first, we examined the expression of laminin α5 that was localized at the basal side of osteopontin$^+$ cholangiocytes in normal liver (Fig. 5*A*, *panel 1*) and confirmed that it was not detected in laminin α5 KO liver (Fig. 5*A*, *panel 2*). On the other hand, laminin α1 was expressed in both the control and mutant livers (Fig. 5*A*, *panels 3* and *4*). Next, we examined the expression of cytokeratin 19 (CK19) to evaluate the differentiation of cholangiocytes from hepatoblasts around the portal vein and revealed that CK19$^+$ cholangiocytes emerged around the portal vein in mutant liver as in the control at E17.5 (Fig. 5*B*). Cholangiocytes in the control and mutant livers were also positive for Sox9 (data not shown). We also examined livers at E16.5 and found CK19$^+$ cells both in the control and mutant livers (data not shown). We further counted CK19$^+$ cells around each portal vein and found that a similar number of CK19$^+$ cells were observed in the control and mutant livers at E17.5 (Fig. 5*C*). Consistent with the normal emergence of cholangiocytes in the KO liver, TGFβ, a major signal inducing the cholangiocytes from hepatoblasts, induced expression of cholangiocyte markers in bipotential hepatoblasts cultured on α1-containing laminin more efficiently than on α5-containing laminin (Fig. 5, *D* and *E*). Thus, α5-containing laminin was dispensable, and α1-containing laminin seemed to be sufficient as an ECM component for the commitment of bipotential hepatoblasts to cholangiocytes.

Loss of Laminin α5 Attenuates Bile Duct Morphogenesis—Next, we compared bile duct structures in laminin α5 KO liver with those in the control. We examined the formation of tight junctions by staining with anti-ZO1 antibody and found that CK19$^+$ cholangiocytes formed tight junctions and surrounded luminal space (Fig. 6*A*), suggesting that apicobasal polarity was established in cholangiocytes in the absence of laminin α5.

On the other hand, it seemed that the lumen of ducts was smaller in laminin α5 KO liver (Fig. 6*A*). We measured the lumen area and found that the lumen size was significantly decreased in laminin α5 KO liver (Fig. 6*B*). Furthermore, the number of duct structures in which CK19$^+$ cholangiocytes completely surrounded the lumen appeared to be fewer in laminin α5 KO liver (Fig. 5*B*, *arrowheads*). On the other hand, immature duct structures in which a lumen was not completely surrounded by CK19$^+$ cholangiocytes (Fig. 6*A*, *panels 9–12*) were more evident in laminin α5 KO liver (supplemental Fig. 6). Therefore, we counted duct structures around each portal vein and found that the number of duct structures was significantly decreased in the mutant liver (Fig. 6*C*). Based on these results, we considered that laminin α5 is required for the formation of mature duct structure during the development of bile ducts.

DISCUSSION

In this study, we showed that, via β1 integrin, liver epithelial cells interacted with α1-containing laminin provided by adjacent fibroblasts while establishing apicobasal polarity and the apical lumen, and subsequently, they produced and utilized α5-containing laminin to further advance bile duct morphogenesis and maintain the structures of bile ducts. Given the fact that renal and submandibular epithelial cells start tubular morphogenesis in the presence of α1-containing laminin, which is later replaced by α5-containing laminin (16, 25), our finding that liver epithelial cells sequentially utilized α1- and α5-containing laminins for distinct processes of bile duct morphogenesis may reflect a general mechanism regulating the formation of tissue structures in epithelial organs.

To clarify sequential contributions of α1- and α5-containing laminins in the development of epithelial tissues, we analyzed structures of bile ducts in laminin α5 KO liver. Consistent with the fact that exogenous α1-containing laminin is necessary for HPPL to develop apicobasal polarity and lumen, α1-containing laminin is sufficient for immature cholangiocytes to establish apicobasal polarity in the absence of laminin α5. However, we found abnormal tubular morphogenesis as shown by the decrease in mature duct structures and reduced size of the remaining ducts in the mutant liver. The reduced number of ducts might result from the delay of tubular morphogenesis. It was reported that ductal plates are converted to mature ducts through an intermediate structure called "asymmetric ducts" (3). Asymmetric ducts could be recognized as lumens surrounded by CK19$^+$HNF4α$^-$ cholangiocytes on one side and

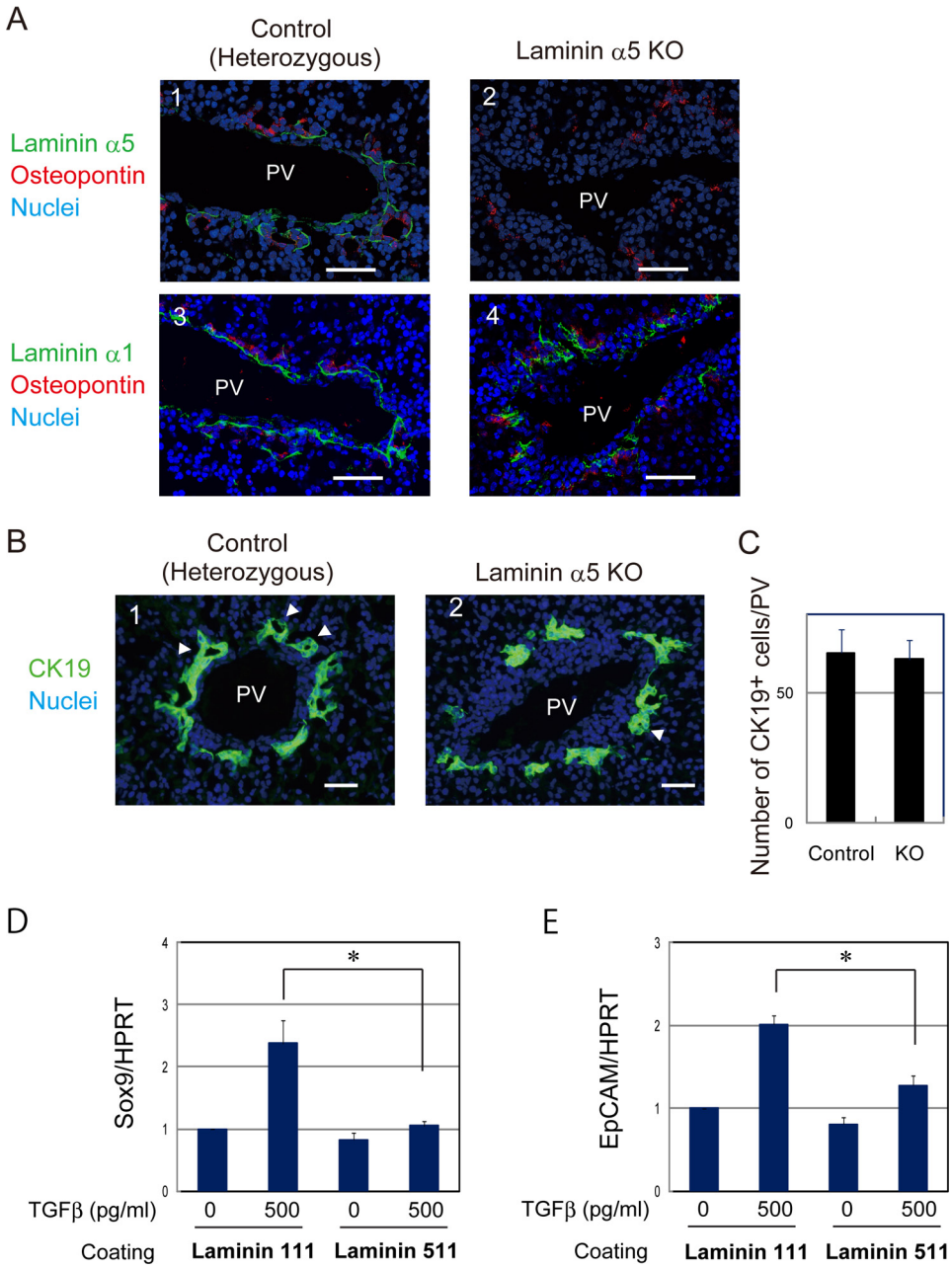

FIGURE 5. **Laminin α5 is dispensable for the lineage determination of hepatoblasts to cholangiocytes.** *A*, laminin α5 is not observed at the basal side of cholangiocytes in laminin α5 KO livers, whereas laminin α1 is normally expressed. The control and laminin α5 KO livers were stained with anti-laminin α5 (*panels 1* and *2*) or anti-laminin α1 (*panels 3* and *4*) and anti-osteopontin antibodies. *Bars* represent 50 μm. *B*, $CK19^+$ cholangiocytes are observed around the portal vein in laminin α5 KO liver. E17.5 liver sections were stained with anti-CK19 antibody. *Arrowheads* indicate luminal structures surrounded by $CK19^+$ cells. *C*, numbers of $CK19^+$ cholangiocytes in the control and mutant livers. The number of $CK19^+$ cholangiocytes around the portal vein was counted in liver sections prepared from two control and three mutant livers. There was no statistically significant difference between the control and KO. A *t* test was performed by Microsoft Excel software. *D* and *E*, TGFβ induces Sox9 and EpCAM, cholangiocyte markers, in hepatoblasts more efficiently on α1-containing laminin than on α5-containing laminin. Hepatoblasts were isolated from E14.5 liver and cultured on dishes coated with α1-containing laminin (laminin 111) or α5-containing laminin (laminin 511). At day 3 of culture, cells were stimulated with 500 pg/ml TGFβ for 24 h. Gene expression was examined by quantitative PCR. Cultures were repeated three times independently. A *t* test was performed by Microsoft Excel software. *, $p < 0.05$. *HPRT*, hypoxanthine phosphoribosyltransferase; *PV*, portal vein. *Error bars* in *panels C*, *D* and *E* represent standard deviation.

$CK19^-HNF4\alpha^+$ hepatoblasts on the other (Fig. 6*A*, *panels 9–12*). We found that the number of asymmetric ducts was increased in the mutant liver (supplemental Fig. 6), suggesting that tubular morphogenesis was attenuated at the middle of the tubular morphogenesis. On the other hand, it is not clear whether the smaller lumen is also caused by the delay of the morphogenesis. In fetal liver, in addition to mature and asymmetric immature ducts, double layered ductal plates associated with or without lumens are observed in late gestation, suggesting that lumens are generated between two layers and gradually increase their size along an alternative morphogenic pathway. Given that laminin α5 contributes to expansion of the luminal space *in vitro*, the lack of laminin α5 in cholangiocytes might reduce the size of lumen, which is generated between ductal plates through this type of morphogenic pathway.

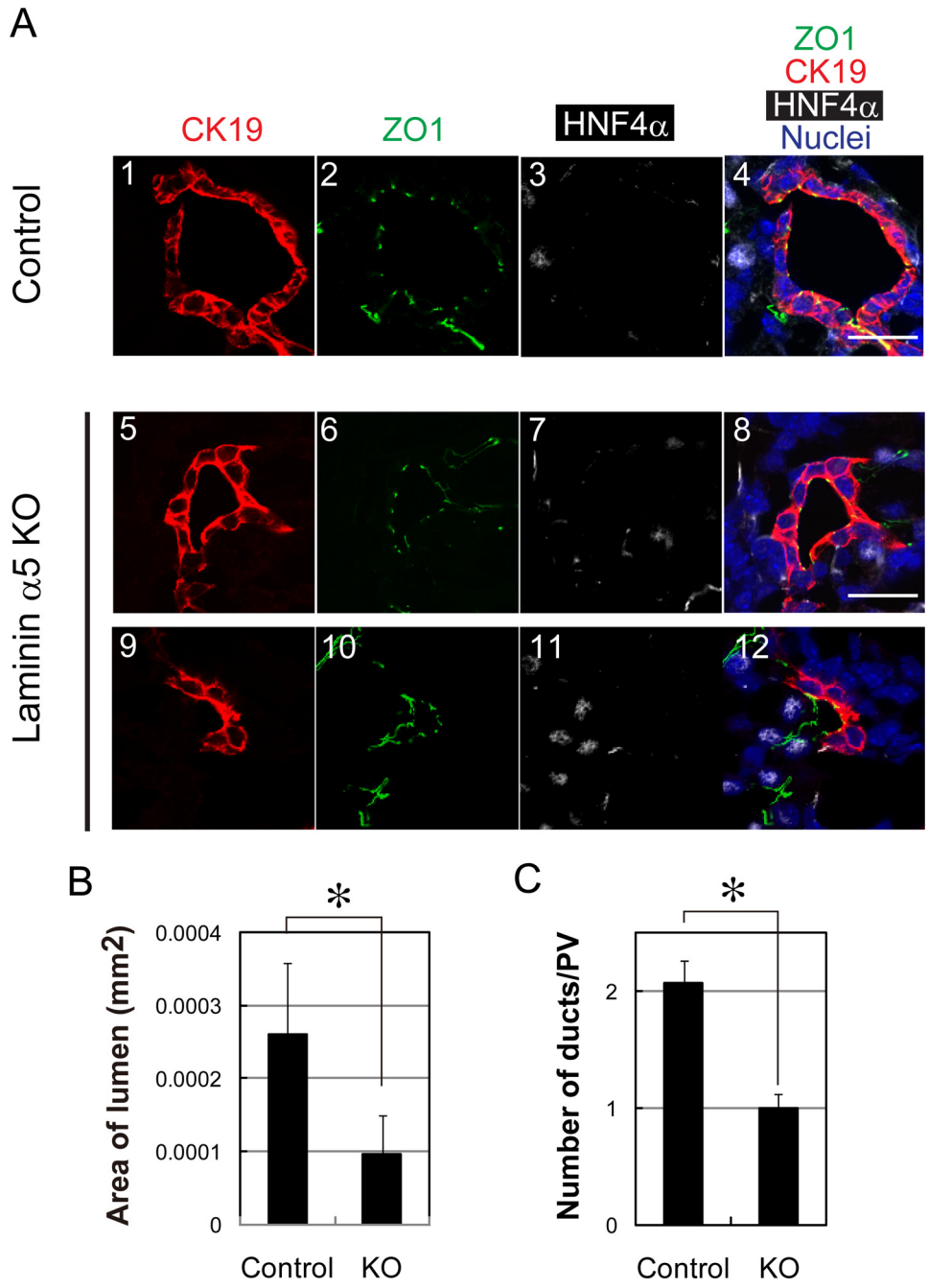

FIGURE 6. **Defects of bile duct formation in laminin α5 KO liver.** *A*, duct structures in the control and laminin α5 KO livers are characterized by the expression of CK19, ZO1, and HNF4α. All three duct structures are associated with a single lumen surrounded by cells with tight junctions recognized by ZO1 staining (*green*). Ducts in *panels 1–8* are totally surrounded by $CK19^+HNF4\alpha^-$ cholangiocytes. On the other hand, an immature duct in *panels 9–12* is surrounded by $CK19^+HNF4\alpha^-$ cholangiocytes and $CK19^-HNF4\alpha^+$ hepatoblasts. *B*, the lumen size of the bile duct is reduced in laminin α5 KO liver. The lumen surrounded with $CK19^+$ cholangiocytes was selected, and its area was measured by ImageJ. A *t* test was performed by Microsoft Excel software. *, $p < 0.05$. *C*, the number of duct structures is reduced in laminin α5 KO liver. $CK19^+$ duct structures around the portal vein were counted in more than 10 sections in each liver tissue. More than 50 portal areas were examined for each embryonic liver. A *t* test was performed by Microsoft Excel software. *, $p < 0.05$. *Scale bars* represent 20 μm. *Error bars* represent standard deviation.

It is known that α1-containing laminin is abundant in fetal tissues but not in adult tissues. By contrast, α5-containing laminin is a major component of basal lamina in mature epithelial tissues. Although laminins α1 and α5 are structurally similar, recent reports demonstrated that α5-containing laminin has some unique functions that cannot be substituted for by α1-containing laminin. Kikkawa and Miner (26) generated laminin α5 KO mice expressing a mutant laminin α5 chain in which the entire α5 laminin globular domain was replaced by α1 laminin globular domain and showed that the mutant laminin α5 chain failed to rescue the developmental defects observed in α5 KO mice. Gao *et al.* (27) demonstrated that α1-containing laminin failed to rescue the defects in hair follicle morphogenesis in laminin α5 KO mice. Our data revealed a novel function of α5-containing laminin in tubular morphogenesis of bile ducts, suggesting that α5-containing laminin

might be involved in epithelial morphogenesis of other epithelial tubular structures in the lung, kidney, reproductive organs, and pancreas.

Our data show that among β1 integrins α6β1 integrin works as a receptor for laminins during cyst morphogenesis of HPPL. In addition to α6, HPPL expresses α3 subunit. Although it remains to be proven that α3 integrin is definitely involved in cyst morphogenesis, because anti-α6 antibody did not completely inhibit cyst morphogenesis, α3 integrin may be another partner of β1 integrin. In contrast to the basal localization of β1 integrin (Fig. 1*A*), β4 integrin in the basal domain was not clear at the beginning of the culture (supplemental Fig. 1A). We also found the expression of β1 integrin in $Sox9^+$ cholangiocytes at E16.5 (supplemental Fig. 2A, arrowheads), whereas most of the $Sox9^+$ cells did not express β4 integrin (supplemental Fig. 2C). These results suggested that β4 integrin signals might be involved in the latter process of bile duct morphogenesis or the maintenance of the structure but not in the establishment of apicobasal polarity. However, β4 integrin signaling is not essential for the maintenance of the cyst structure because anti-β4 antibody only slightly disrupted the cyst structure (supplemental Fig. 1C). Thus, β1 integrin mainly mediates signals from laminins in HPPL during and after the cyst formation in three-dimensional culture.

β1 integrin has been shown to play important roles for epithelial cells to receive ECM signals (15–19). Blocking the function of β1 integrin resulted in dissolution of the cyst structure, but the polarity was not completely dissolved; the apical markers were not randomly localized but faced the ECM, and tight junctions were formed at cell-cell contacts near the ECM. A similar phenotype has been described in three-dimensional culture of Madin-Darby canine kidney cells (15, 28) and in the *Drosophila* ovary (29) and is considered to be "inverted polarity." However, in the culture of HPPL, anti-β1 integrin induced inverted polarity in the presence of exogenous laminin. By contrast, Madin-Darby canine kidney cells could form the normal apicobasal polarity by the addition of exogenous laminin even in the presence of anti-β1 antibody. The difference might be explained by the fact that Madin-Darby canine kidney cells may express an unknown laminin receptor that is not expressed in HPPL.

In summary, we have demonstrated that the formation of apicobasal polarity and lumen, progression of tubular morphogenesis, and maintenance of the proper bile duct structure require signaling by β1 integrin that is sequentially activated by α1-containing laminin provided via mesenchymal cells and then α5-containing laminin expressed by cholangiocytes themselves. It was reported that laminin and type IV collagen, two major components of the basal lamina, were reduced or partly lost around bile ducts in congenital hepatic fibrosis and Caroli disease and in the PCK rat liver, an animal model of Caroli disease (30). Thus, the interactions between laminin and cholangiocytes may also be important for preventing the pathogenesis of fibrosis. However, it has remained unknown how the degeneration of the basal lamina leads to fibrosis. In three-dimensional culture, the layer of basal laminin was disrupted in parallel with the loss of polarity (supplemental Fig. 7). By inhibiting the interaction between ECM and epithelial cells in three-dimensional culture of HPPL, it may be possible to obtain critical information on the link between the loss of integrity of the basal lamina and the pathogenesis of fibrosis in epithelial tissues.

Acknowledgments—We thank Dr. Takako Sasaki for providing antibodies against laminins α1 and α5. We also thank Dr. Jeff H. Miner for providing liver tissues of laminin α5 KO mice. We appreciate the valuable technical assistance of Shigeru Saito, Minako Kuwano, and Yumiko Tsukamoto. We thank the members of the laboratories of Prof. Miyajima and Prof. Mitaka for helpful discussions.

REFERENCES

1. Shiojiri, N. (1997) Development and differentiation of bile ducts in the mammalian liver. *Microsc. Res. Tech.* **39,** 328–335
2. Lemaigre, F. P. (2003) Development of the biliary tract. *Mech. Dev.* **120,** 81–87
3. Antoniou, A., Raynaud, P., Cordi, S., Zong, Y., Tronche, F., Stanger, B. Z., Jacquemin, P., Pierreux, C. E., Clotman, F., and Lemaigre, F. P. (2009) Intrahepatic bile ducts develop according to a new mode of tubulogenesis regulated by the transcription factor SOX9. *Gastroenterology* **136,** 2325–2333
4. Zong, Y., Panikkar, A., Xu, J., Antoniou, A., Raynaud, P., Lemaigre, F., and Stanger, B. Z. (2009) Notch signaling controls liver development by regulating biliary differentiation. *Development* **136,** 1727–1739
5. Sanzen, T., Harada, K., Yasoshima, M., Kawamura, Y., Ishibashi, M., and Nakanuma, Y. (2001) Polycystic kidney rat is a novel animal model of Caroli's disease associated with congenital hepatic fibrosis. *Am. J. Pathol.* **158,** 1605–1612
6. Martin-Belmonte, F., Gassama, A., Datta, A., Yu, W., Rescher, U., Gerke, V., and Mostov, K. (2007) PTEN-mediated apical segregation of phosphoinositides controls epithelial morphogenesis through Cdc42. *Cell* **128,** 383–397
7. Kesavan, G., Sand, F. W., Greiner, T. U., Johansson, J. K., Kobberup, S., Wu, X., Brakebusch, C., and Semb, H. (2009) Cdc42-mediated tubulogenesis controls cell specification. *Cell* **139,** 791–801
8. Colognato, H., and Yurchenco, P. D. (2000) Form and function: the laminin family of heterotrimers. *Dev. Dyn.* **218,** 213–234
9. Miner, J. H., and Yurchenco, P. D. (2004) Laminin functions in tissue morphogenesis. *Annu. Rev. Cell Dev. Biol.* **20,** 255–284
10. Durbeej, M. (2010) Laminins. *Cell Tissue Res.* **339,** 259–268
11. Kikkawa, Y., Mochizuki, Y., Miner, J. H., and Mitaka, T. (2005) Transient expression of laminin α1 chain in regenerating murine liver: restricted localization of laminin chains and nidogen-1. *Exp. Cell Res.* **305,** 99–109
12. Kikkawa, Y., Sudo, R., Kon, J., Mizuguchi, T., Nomizu, M., Hirata, K., and Mitaka, T. (2008) Laminin α5 mediates ectopic adhesion of hepatocellular carcinoma through integrins and/or Lutheran/basal cell adhesion molecule. *Exp. Cell Res.* **314,** 2579–2590
13. Shiojiri, N., and Sugiyama, Y. (2004) Immunolocalization of extracellular matrix components and integrins during mouse liver development. *Hepatology* **40,** 346–355
14. Tanimizu, N., Miyajima, A., and Mostov, K. E. (2007) Liver progenitor cells develop cholangiocyte-type epithelial polarity in three-dimensional culture. *Mol. Biol. Cell* **18,** 1472–1479
15. Yu, W., Datta, A., Leroy, P., O'Brien, L. E., Mak, G., Jou, T. S., Matlin, K. S., Mostov, K. E., and Zegers, M. M. (2005) β1-integrin orients epithelial polarity via Rac1 and laminin. *Mol. Biol. Cell* **16,** 433–445
16. Rebustini, I. T., Patel, V. N., Stewart, J. S., Layvey, A., Georges-Labouesse, E., Miner, J. H., and Hoffman, M. P. (2007) Laminin α5 is necessary for submandibular gland epithelial morphogenesis and influences FGFR expression through β1 integrin signaling. *Dev. Biol.* **308,** 15–29
17. Zhang, X., Mernaugh, G., Yang, D. H., Gewin, L., Srichai, M. B., Harris, R. C., Iturregui, J. M., Nelson, R. D., Kohan, D. E., Abrahamson, D., Fässler, R., Yurchenco, P., Pozzi, A., and Zent, R. (2009) β1 integrin is necessary for ureteric bud branching morphogenesis and maintenance of collecting

duct structural integrity. *Development* **136,** 3357–3366
18. Bombardelli, L., Carpenter, E. S., Wu, A. P., Alston, N., DelGiorno, K. E., and Crawford, H. C. (2010) Pancreas-specific ablation of β1 integrin induces tissue degeneration by disrupting acinar cell polarity. *Gastroenterology* **138,** 2531–2540, 2540.e1–4
19. Myllymaki, S. M., Teräväinen, T. P., and Manninen, A. (2011) Two distinct integrin-mediated mechanisms contribute to apical lumen formation in epithelial cells. *PLoS One* **6,** e19453
20. Kikkawa, Y., Sasaki, T., Nguyen, M. T., Nomizu, M., Mitaka, T., and Miner, J. H. (2007) The LG1–3 tandem of laminin α5 harbors the binding sites of Lutheran/basal cell adhesion molecule and α3β1/α6β1 integrins. *J. Biol. Chem.* **282,** 14853–14860
21. Tanimizu, N., Nishikawa, M., Saito, H., Tsujimura, T., and Miyajima, A. (2003) Isolation of hepatoblasts based on the expression of Dlk/Pref-1. *J. Cell Sci.* **116,** 1775–1786
22. Tanaka, M., Okabe, M., Suzuki, K., Kamiya, Y., Tsukahara, Y., Saito, S., and Miyajima, A. (2009) Mouse hepatoblasts at distinct developmental stages are characterized by expression of EpCAM and DLK1: drastic change of EpCAM expression during liver development. *Mech. Dev.* **126,** 665–676
23. Suzuki, K., Tanaka, M., Watanabe, N., Saito, S., Nonaka, H., and Miyajima, A. (2008) p75 neurotrophin receptor is a marker for precursors of stellate cells and portal fibroblasts in mouse fetal liver. *Gastroenterology* **135,** 270–281.e3
24. Okabe, M., Tsukahara, Y., Tanaka, M., Suzuki, K., Saito, S., Kamiya, Y., Tsujimura, T., Nakamura, K., and Miyajima, A. (2009) Potential hepatic stem cells reside in $EpCAM^+$ cells of normal and injured mouse liver. *Development* **136,** 1951–1960
25. Sorokin, L. M., Pausch, F., Durbeej, M., and Ekblom, P. (1997) Differential expression of five laminin α (1–5) chains in developing and adult mouse kidney. *Dev. Dyn.* **210,** 446–462
26. Kikkawa, Y., and Miner, J. H. (2006) Molecular dissection of laminin α5 *in vivo* reveals separable domain-specific roles in embryonic development and kidney function. *Dev. Biol.* **296,** 265–277
27. Gao, J., DeRouen, M. C., Chen, C. H., Nguyen, M., Nguyen, N. T., Ido, H., Harada, K., Sekiguchi, K., Morgan, B. A., Miner, J. H., Oro, A. E., and Marinkovich, M. P. (2008) Laminin-511 is an epithelial message promoting dermal papilla development and function during early hair morphogenesis. *Genes Dev.* **22,** 2111–2124
28. Yu, W., Shewan, A. M., Brakeman, P., Eastburn, D. J., Datta, A., Bryant, D. M., Fan, Q. W., Weiss, W. A., Zegers, M. M., and Mostov, K. E. (2008) Involvement of RhoA, ROCK I and myosin II in inverted orientation of epithelial polarity. *EMBO Rep.* **9,** 923–929
29. Fernández-Miñán, A., Cobreros, L., González-Reyes, A., and Martín-Bermudo, M. D. (2008) Integrins contribute to the establishment and maintenance of cell polarity in the follicular epithelium of the *Drosophila* ovary. *Int. J. Dev. Biol.* **52,** 925–932
30. Yasoshima, M., Sato, Y., Furubo, S., Kizawa, K., Sanzen, T., Ozaki, S., Harada, K., and Nakanuma, Y. (2009) Matrix proteins of basement membrane of intrahepatic bile ducts are degraded in congenital hepatic fibrosis and Caroli's disease. *J. Pathol.* **217,** 442–451